ORIGINAL ARTICLE

High-fat Diet and Low-dose Streptozotocin-Induced Type 2 Diabetes: *In Silico* and *in Vivo* Study of Heterocyclic Derivatives

Shital S. Phadtare, Vitthal V. Chopade

Department of Pharmaceutical Chemistry, PES Modern College of Pharmacy, Savitribai Phule Pune University, Pune, Maharashtra, India

Abstract

Aim: The present study aimed to design and evaluate novel heterocyclic derivatives for their antidiabetic potential using *in silico* molecular docking and *in vivo* evaluation in a high-fat diet (HFD) and low-dose streptozotocin (STZ)–induced type 2 diabetic rat model. **Material and Methods:** *In silico* molecular docking was performed to assess the binding affinity and interaction patterns of the heterocyclic derivatives with the dipeptidyl peptidase-4 (DPP-4) enzyme. For *in vivo* evaluation, type 2 diabetes mellitus (T2DM) was induced in rats by feeding an HFD followed by administration of low-dose STZ. Antidiabetic activity was assessed using fasting blood glucose levels and oral glucose tolerance test (OGTT). **Results and Discussion:** Molecular docking studies revealed strong binding interactions of selected heterocyclic derivatives with key active-site residues of the DPP-4 enzyme. *In vivo* studies demonstrated a significant reduction in fasting blood glucose levels and a marked improvement in glucose tolerance in treated groups compared with diabetic control animals. **Conclusion:** The combined *in silico* and *in vivo* findings indicate that the designed heterocyclic derivatives exhibit promising antidiabetic activity in the HFD/STZ-induced type 2 diabetes model and may serve as potential lead compounds for further drug development.

Key words: Type 2 diabetes mellitus, High-fat diet, Streptozotocin, Heterocyclic derivatives, Molecular docking, DPP-4 inhibitor

INTRODUCTION

Non-insulin-dependent diabetes is an increasing cellular metabolism disorder involving decreased insulin effectiveness and declining insulin-producing pancreatic beta cells. It comprises nearly 90–95% of all reported diabetes patients and has become a leading, rapidly increasing major worldwide health issue. Sedentary lifestyles, obesity, and dietary patterns rich in fats have a major effect on the rising complications in non-insulin-dependent diabetes.[1] Despite the availability of several antidiabetic agents, many current therapies exhibit limitations such as side effects, reduced efficacy with long-term use, or poor patient compliance. Therefore, the discovery of safer and more effective therapeutic molecules remains a key priority in diabetes research. Experimental animal models play an essential role in understanding diabetes pathophysiology and evaluating novel therapeutic agents. Among the various models available, the induction method employing high-fat diet (HFD) intake before low-dose streptozotocin (STZ) administration has gained substantial recognition for mimicking human type 2 diabetes mellitus (T2DM). The HFD and low-dose STZ model has become among the leading widely accepted animal models for replicating the dual-defect nature of type 2 diabetes. HFD promotes obesity and insulin resistance, while low-dose STZ induces partial β-cell dysfunction, collectively reproducing the metabolic and biochemical alterations associated with

Address for correspondence:
Shital S Phadtare, PES Modern College of Pharmacy, Savitribai Phule Pune University, Nigdi, Pune, Maharashtra, India. Phone: 7972109692.
E-mail: phadtareshital18@gmail.com

Received: 28-08-2025
Revised: 20-10-2025
Accepted: 31-12-2025

T2DM progression. This model offers high reproducibility, stable hyperglycemia, and close clinical resemblance to human conditions, making it ideal for pharmacological investigations.[2-4] In parallel, computational (*in silico*) drug-discovery approaches have become powerful tools for predicting biological activity, identifying molecular targets, and screening large numbers of compounds with minimal cost and time. Heterocyclic derivatives, which represent a major class of biologically active molecules, have demonstrated a significant potential as antidiabetic agents due to their structural diversity and strong interactions with key metabolic enzymes. Molecular docking and absorption, distribution, metabolism, excretion, toxicity (ADMET) prediction help in understanding their binding affinities, pharmacokinetic properties, and therapeutic suitability. The present study integrates both *in vivo* and *in silico* approaches to explore the antidiabetic potential of selected heterocyclic derivatives. The HFD + low-dose STZ rat model was employed to induce T2DM and evaluate biological responses, while computational techniques were used to assess compound–protein interactions and drug-likeness properties. This combined approach aims to identify promising heterocyclic derivatives with potential for further development as effective antidiabetic agents.

IMATERIALS AND METHODS

Molecular docking software

Protein retrieval Protein PDB code (2ONC)

The three-dimensional atomic configuration of the target protein 2ONC was imported from the protein data bank (PDB) and uploaded into Maestro.[5,6]

Protein optimization

The framework of the protein was processed using the Protein Preparation Wizard (OPLS4 force field). Processing steps included: assigning bond orders, adding missing hydrogen atoms, correcting formal charges, capping termini where required, modeling missing side-chains/loops (if present), deleting crystallographic waters beyond 5.0 Å from the ligand-binding site, and optimizing protonation states at pH 7.4 ± 0.2. A restrained minimization was performed with a root mean square deviation convergence cutoff of 0.3 Å.

Identification of the binding site

The active site was identified by inspection of the co-crystallized ligand and using site map/literature information to confirm the pocket. A receptor grid was centered on the identified active site residues to encompass the binding cavity.

Ligand preparation (LigPrep)

Ligands were processed with LigPrep: 2D → 3D conversion, ionization and protonation state generation at pH 7.4 ± 0.2, tautomer and stereoisomer enumeration where applicable, and energy minimization optimized through the OPLS4 parameter set.[7,8]

Generation of receptor interaction grid

The Glide grid-generation workflow was utilized to obtain the receptor grid file. The grid box was defined to encompass the active site of the protein; van der Waals radii scaling (ligand and receptor) and constraints (if needed on key residues) were applied to reflect known interactions.

Docking protocol (glide)

Docking was performed using Glide with a hierarchical approach: First, high-throughput virtual screening (if a large library), then Standard Precision (SP) for the filtered set, and Extra Precision (XP) for top-ranked compounds. Settings: Flexible ligand sampling, up to 10 poses saved per ligand, and default glide score ranking. Where required, positional constraints were applied to preserve interactions with key catalytic residues.[9,10]

Analysis of docking results

Docking poses were analyzed in Maestro using 3D visualization and 2D interaction diagrams. Key interactions (hydrogen bonds, π–π stacking, hydrophobic contacts, salt bridges) between heterocyclic derivatives and 2ONC active-site residues were recorded. The best binding conformations were selected based on the glide score.[11]

ADMET prediction

Molecular properties govern the behavior of compounds during design, optimization, and synthesis; their prediction is a vital component of the drug advancement process. The drug likeness score, molecular properties, and *in silico* absorption, distribution, metabolism, excretion data predictions of the designed molecules have been predicted using freely available web-based applications, such as the Structural Assessment Prediction Tool (*http://www.molsoft.com/mprop/*) and for ADMET data, Pre-ADMET (*http://preadmet.bmdrc.org/*). The tool was used to screen various pharmacokinetic properties of derivatives such as carboxymethylcellulose (CMC)-like rule, Lipinski's rule, central nervous system (CNS) accessibility, plasma protein affinity, $Caco_2$ cell permeability, human intestinal absorption (HIA), and skin permeability.[12-14]

Prediction of toxicity

The Protox 3.0 tool was employed to estimate the toxicity of heterocyclic derivatives,[15] which includes organ toxicities such as hepatotoxicity, carcinogenicity, mutagenicity, cytotoxicity, and immunogenicity.

Biological activity

Animals

After approval from the Animal Ethical Committee (MCP/IAEC/017/2025), the Antihyperglycemic activity study was carried out. Swiss albino mice (20–30 g) were used for the toxicity investigation, weighing 20–30 g and for antidiabetic activity screening, Sprague–Dawley rats weighing between 120 and 150 g were obtained from Crystal Biological Solutions, Uruli Devachi, Pune, India. The animals were maintained in an accepted laboratory environment with ad libitum access to a normal diet and clean drinking water. Environmental conditions such as room temperature, ventilation, and a 12-h illumination and 12-h darkness rotation were carefully maintained throughout the study. Before the start of the study, all animals were placed under fasting conditions for 16 h while being allowed water *ad libitum*. All procedures conducted in this experiment complied with the regulations of the Committee for Monitoring and Governance of Experiments on Animals (CPCSEA), Government of India, under registration number 884/PO/Re/S/05/CPCSEA, and received approval from the Institutional Animal Ethics Committee.

Acute toxicity through the oral route (OECD 423)

Toxicity testing was conducted in accordance with OECD Test Guideline 423, which outlines the acute oral toxicity – acute toxic class methodology. Swiss albino mice (20–30 g) were fasted for 3–4 h before dosing, with access to water, and their body weights were recorded. The test compounds were formulated as 0.5% sodium CMC-Na suspensions and delivered orally to the animals. By gavage at predetermined doses of 5, 50, 300, and 2000 mg/kg in accordance with the stepwise acute toxicity procedure (three animals per level). A maximum tolerated dose of 2000 mg/kg was also evaluated to confirm the toxicity profile. Animals were observed continuously for the 1st 4 h post-dose, then daily for 14 days, to monitor clinical signs, behavioral changes, body weight, food, and water consumption. For the acute oral toxicity assessment of the test compounds, a maximum tolerated dose of 2000 mg/kg animal weight was delivered to the experimental rats. Throughout the LD_{50} evaluation, the animals exhibited normal behavior with no signs of toxicity or mortality at this maximum dose. These observations align with the criteria outlined in OECD Guideline 423.[16]

Induction of diabetes

HFD providing 60% of caloric intake was prepared with the following composition: 2.0 g/kg cholesterol, 8.0 g/kg concentrated fat (peanut oil), and 0.1 g/kg calcium. Rats were maintained on this HFD along with a once-weekly oral administration of Vitamin D_3 (300,000 IU) for an early phase of 2 weeks. The detailed formulation of the dietary components is presented in Table 1. At day 14, the animals were fasted for 12 h and subsequently administered STZ (35 mg/kg, i.p.) dissolved in 0.1 M cold citrate buffer (pH 4.5). Treatment with the test compounds commenced 14 days after STZ administration, which was designated as Day 1 of the study, and continued for 2 weeks.

Antihyperglycemic activity

Animals with blood glucose concentrations above 250 mg/dL were considered hyperglycemic and selected for antidiabetic evaluation. Blood was sampled from the retro-orbital region for biomolecular analysis. Upon completion of the acclimation period, all animals were randomly divided into 25 groups for the study duration.

Experimental procedure

- Group I: Normal control animals received physiological saline
- Group II: Disease control animals were administered the HFD/STZ regimen
- Group III: HFD/STZ-induced diabetic rats were administered alogliptin (20 mg/kg) as the standard reference drug to assess comparative efficacy
- Test Groups IV: Animals in the test groups (S1R1-S1R11 and S2R1-S2R11) received the selected dose of 45 mg/kg of the respective test compounds.

Glucose level in blood was recorded at 0–8 h at 1-h intervals using Glucometer (BG-03) and compatible test strips, with specimens obtained through the retro-orbital plexus. The percentage reduction in blood glucose concentration from 0 to 8 h was calculated for each test compound to determine its antihyperglycemic effect.

Determination of fasting blood glucose level (FBGL)

Only two compounds, S1R7 and S2R7, were selected for further investigation, based on their biological responses observed during the preliminary screening. FBGL were assessed in all experimental animals at the start of the study to establish baseline diabetic status. The same procedure was

Table 1: Dietary components of HFD

S. No.	Dietary components	Quantity (g/kg)
1	Fat	22
2	Carbohydrate	48
3	Protein	20
4	Vitamin	4.9
5	Fat	6.6
6	Total calorie	44.3

HFD: High-fat diet

repeated once per week throughout the 28-day treatment schedule. After an overnight fast, blood samples were obtained through the retro-orbital sinus, and glucose concentrations were immediately recorded using a Glucometer (BG-03) and compatible test strips.[17]

Oral glucose tolerance test (OGTT)

At day 28th of the treatment schedule, glucose tolerance assessment through the oral route was performed on all groups. Following an overnight fast, a baseline blood sample (0 min) was sampled from the retro-orbital sinus of normal along diabetic rats to determine their initial glucose levels. Immediately thereafter, an oral glucose load was administered. Additional blood specimens were drawn from the retro-orbital sinus, recorded at 15–120 min at defined intervals following glucose administration, and glucose concentrations were determined using a glucometer (BG-03) and compatible test strips.[18]

Statistical evaluation

The experimental results were presented as the mean ± standard error of the mean. IC_{50} data were calculated through non-linear modeling. Group-wise comparisons were performed using single-factor analysis of variance followed by Dunnett's *post hoc* test. The entire data evaluation was performed with Prism software (GraphPad Version 10).

RESULTS AND DISCUSSION

In silico docking

Ligand–protein docking and ADMET prediction were employed to examine the functional characteristics. A dimeric dipeptidyl peptidase-IV (DPP-IV) protein (PDB ID: 2ONC), with a crystallographic clarity of 2.55 Å, was selected as the target for molecular docking studies. The binding site residues from chain A were analyzed to identify the active pocket and interaction hotspots essential for ligand binding. 2ONC is the only crystallized human DPP-IV complex currently available, and therefore, it was selected as the structural basis for this study. It was bound to SY1 800(A). A more negative binding energy reflects a more stable predicted binding strength of the ligand for the active target. Among the derivatives, S2R7 and S2R11 exhibited the highest negative binding score of −9.58 kcal/mol and −9.43, indicating strong binding affinity toward the DPP-IV enzyme. The compound interacted with key active site amino acid residues, including ARG:125, TYR:662, TYR:666, and HIS:740. In comparison, the reference drug alogliptin showed a lower negative binding docking score of −7.30 kcal/mol and built a connection with residues ARG:125, GLU:206, TYR:631, and TYR:666. Docking scores are summarized in Table 2. The remaining compounds also show strong binding affinities comparable to that of the reference inhibitor alogliptin for the DPP-IV enzyme. Table 3 illustrates the 2D and 3D interaction profiles of the selected compounds, along with the corresponding amino acid residues involved in binding and their docking scores. Table 3 illustrates that the 2D interaction diagrams provide a clear view of hydrogen bonds, hydrophobic interactions, and aromatic stacking, while 3D representations depict the spatial orientation of each ligand within the active site pocket. The listed amino acid residues highlight the key points of contact responsible for stabilizing the ligand–receptor complex. In addition, the binding energy values offer a quantitative measure of affinity, enabling comparison of the compounds based on their interaction strength. This combined visual and numerical analysis helps in identifying the most promising derivatives with strong and specific binding toward the protein target.

Screening of heterocyclic derivatives through ADMET analysis

Table 4 summarizes the ADMET evaluation of the heterocyclic derivatives, showing that most compounds possess favorable pharmacokinetic and safety profiles. The results indicate good absorption, acceptable metabolic stability, and low predicted toxicity, suggesting that these derivatives exhibit a promising overall drug-like behavior. The evaluated heterocyclic derivatives exhibited favorable drug-like properties and pharmacokinetic profiles across multiple ADMET parameters. All compounds complied with both the CMC-like rule and Lipinski's Rule of 5, confirming acceptable physicochemical characteristics and good oral bioavailability. High Caco-2 permeability and elevated HIA (%) values reflected strong intestinal absorption, while moderate plasma protein binding ensured sufficient free drug concentration in systemic circulation. Low blood–brain barrier penetration suggested minimal potential for

Table 2: Molecular docking score of heterocyclic compounds against the DPP-4 enzyme (PDB:3ONC)

Compound code	Binding affinity (Kcal/mol)
S2R1	−9.347
S2R2	−9.148
S2R3	−9.090
S2R4	−8.608
S2R5	−9.098
S2R6	−9.079
S2R7	−9.583
S2R8	−9.070
S2R9	−9.034
S2R10	−9.052
S2R11	−9.435
Alogliptin	−7.308

DPP-4: Dipeptidyl peptidase-4

Table 3: Molecular interactions of heterocyclic derivatives with the DPP-4 target protein (PDB ID: 2ONC)

Compound code	Structure	2D interaction	3D interaction	Binding energy (Kcal/mol)	Active site amino acids
S2R1	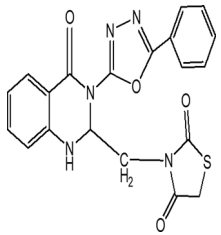	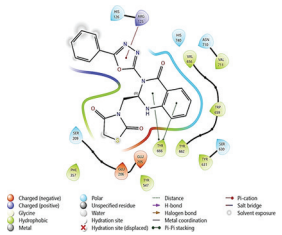	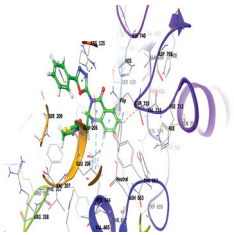	−9.347	ARG:125,GLU:205,GLU:206,VAL:656,TYR:662, TYR:666
S2R2	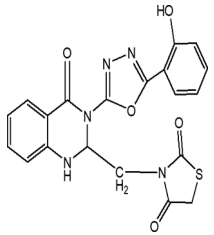	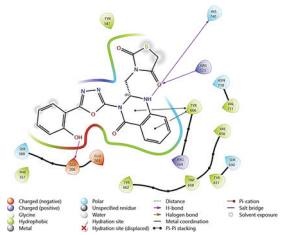	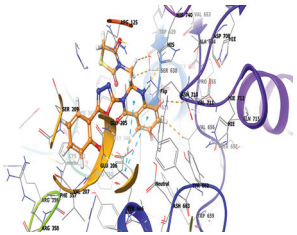	−9.148	ARG:125,GLU:205,GLU:206,TYR:666,ARG:669, HIS:740
S2R3	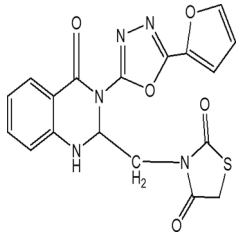	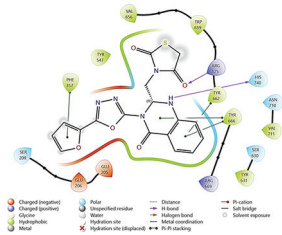	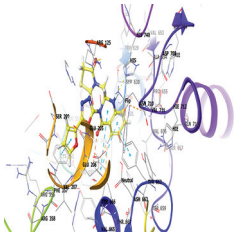	−9.00	ARG:125GLU:205,PHE:357,TYR:662,TYR:666, HIS:740
S2R4	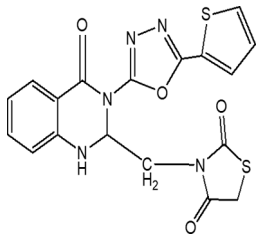		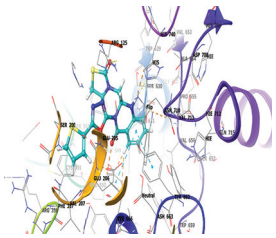	−8.608	ARG:125,GLU:206,TYR:662,TYR:666,HIS:740

(*Contd...*)

Table 3: (*Continued*)

Compound code	Structure	2D interaction	3D interaction	Binding energy (Kcal/mol)	Active site amino acids
S2R5	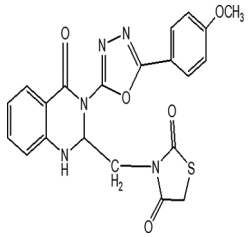	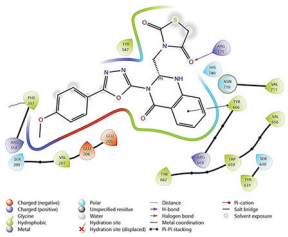	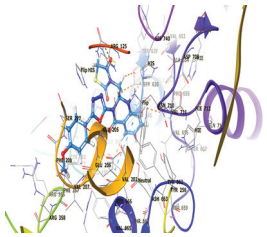	−9.098	ARG:125,GLU:205,TYR:659,TYR:666
S2R6	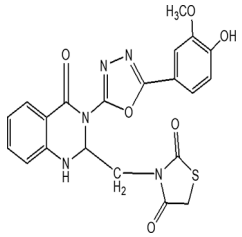	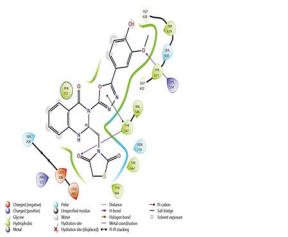	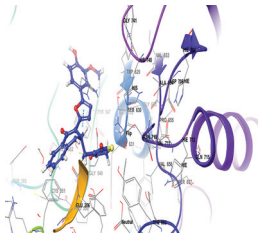	−9.079	GLU:205,TYR:547,LYS:554
S2R7	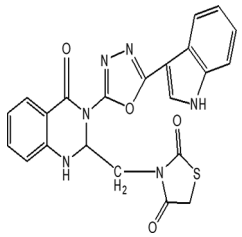	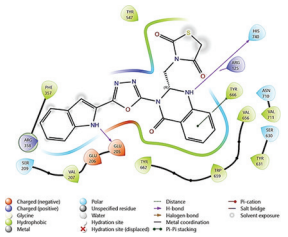	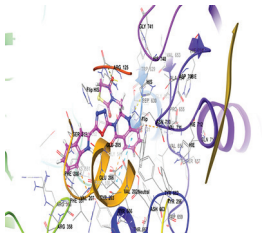	−9.583	ARG:125,GLU205,TYR:662,TYR:666,HIS:740
S2R8	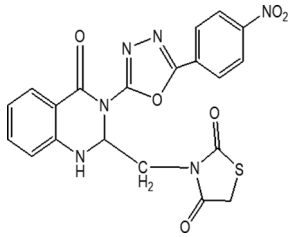	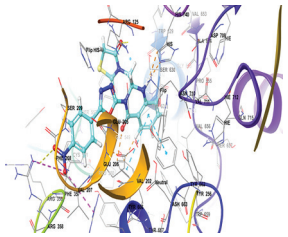	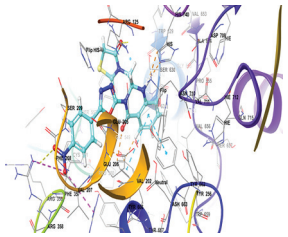	−9.070	ARG:125,ARG:358,TYR:662,TYR:666,ARG:669

(*Contd...*)

Table 3: (*Continued*)

Compound code	Structure	2D interaction	3D interaction	Binding energy (Kcal/mol)	Active site amino acids
S2R9	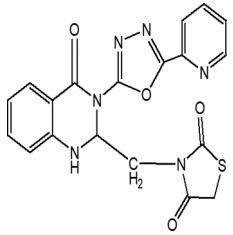	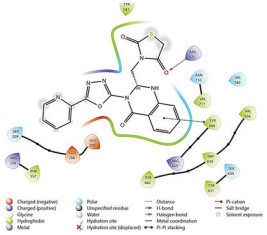	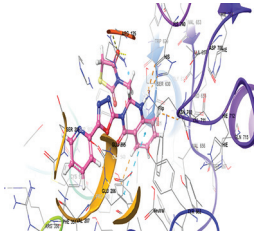	−9.034	ARG:125,GLU:205,TYR:662,TYR:666
S2R10	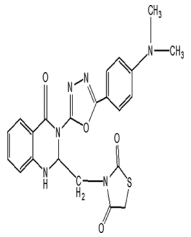	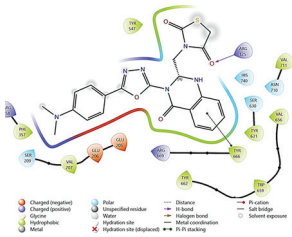	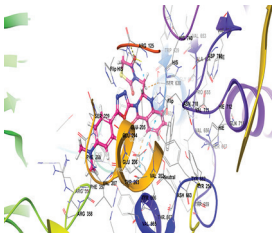	−9.052	ARG:125,GLU:206,TYR:631,TYR:666
S2R11	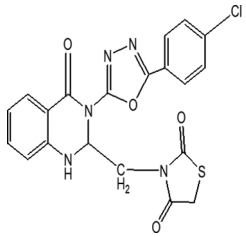	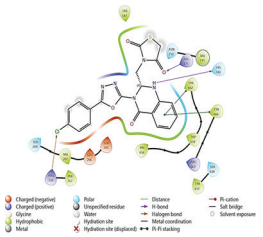	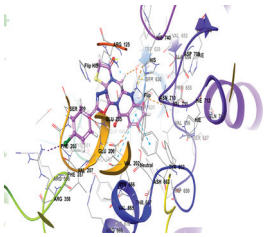	−9.435	ARG:125,ARG:359,TYR:662,TYR:666,HIS:740
Alogliptin	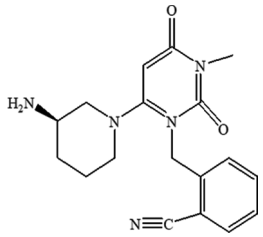	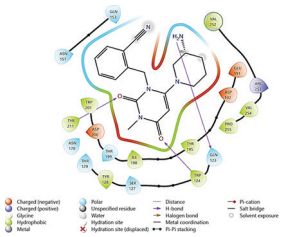	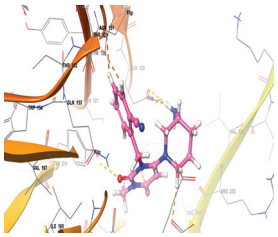	−7.308	ARG:125,GLU:205,GLU:206,PHE:357, TYR:547,TYR:631TYR:662,TYR:666

DPP-4: Dipeptidyl peptidase-4, PDB: Protein data bank

Table 4: ADMET properties of the heterocyclic derivatives

Compound	S2R1	S2R2	S2R3	S2R4	S2R5	S2R6	S2R7	S2R8	S2R9	S2R10	S2R11
CMC-like rule	0.92	0.71	0.82	0.91	0.82	0.93	0.91	0.92	0.88	0.89	0.98
Rule of 5	1	1	1	1	1	1	1	1	1	1	1
BBB	−0.126	−0.117	−0.13	−0.221	−0.214	−0.321	−0.2597	−0.3215	−0.2365	−0.1456	−0.1239
$CaCO_2$ nm/s^2	151	154	155	158	155	161	159	160	157	162	164
HIA%	95.91	93.12	97.46	94.12	93.01	95.13	94.16	95.52	95.79	94.26	94.47
PPB	94.80	91.15	96.24	90.26	95.16	97.15	94.32	96.73	91.65	95.65	95.98
Skin permeability	−2.02	−2.56	−3.21	−2.31	−2.16	−3.85	−2.56	−1.45	−3.74	−2.37	−1.83
Ames test	Non-mutagen	Non-mutagen	Non-mutagen	Non-mutagen	Non-mutagen	Non-mutagen	Non-mutagen	Non-mutagen	Non-mutagen	Non-mutagen	Non-mutagen
Carcino mouse	Negative	Negative	Negative	Negative	Positive	Negative	Negative	Positive	Negative	Negative	Positive
Caecino rat	Negative	Negative	Negative	Negative	Negative	Negative	Negative	Negative	Positive	Negative	Negative
mol log p	3.11	3.28	2.27	1.85	3.56	1.40	2.31	3.45	2.16	3.06	3.04
H Bond donor	2	2	2	2	2	2	2	2	1	2	2
H Bond acceptor	8	9	8	9	7	8	8	7	9	8	8
Drug likeness score	0.92	0.95	0.89	0.97	0.91	0.94	0.88	0.79	0.89	0.87	0.92
CYP2C19/ CYP2D6 inhibitor	No	No	No	No	No	No	No	No	No	No	No
MDCK permeability	155	164	158	157	169	168	163	162	162	150	159
SKlogD (pH)	2	2.5	3	2	2.5	3	2	2	3	2.5	2

ADMET: Absorption, distribution, metabolism, excretion, toxicity, CMC: Carboxymethylcellulose, BBB: Blood-brain barrier, HIA: Human intestinal absorption, PPB: Plasma Protein Binding

CNS effects. The derivatives also demonstrated acceptable skin permeability, supporting efficient membrane diffusion. Toxicity predictions showed a negative Ames test results and non-carcinogenic behavior in both mouse and rat models, highlighting a strong safety profile. Optimal Mol LogP values, along with appropriate hydrogen bond donor and acceptor counts, indicated balanced lipophilicity and good interaction capability. High drug-likeness scores further supported their suitability as drug candidates. In addition, the compounds were not predicted to inhibit CYP2C19 or CYP2D6 enzymes, reducing the likelihood of drug–drug interactions. High Madin-Darby Canine kidney (cells) (MDCK) permeability and favorable SKlogD values confirmed efficient transport and optimal lipophilicity at physiological pH, collectively indicating that these heterocyclic derivatives possess a robust and well-balanced ADMET profile suitable for further development.

Toxicity prediction

Table 5 presents the toxicity assessment of the heterocyclic derivatives, demonstrating that the tested compounds are within a safe toxicity range with predicted oral LD_{50} values exceeding 2000 mg/kg, placing them in Toxicity Class 5. The predictions further suggested that the molecules are non-hepatotoxic, showing no likelihood of liver damage. In addition, the derivatives were classified as non-carcinogenic and non-mutagenic, implying a minimal probability of inducing cancer or causing genetic alterations. Overall, the toxicity profile supports the safe nature of these heterocyclic derivatives for further pharmacological evaluation.

Biological activity

The results of the acute oral toxicity (OECD 423) assessment indicate that the test compounds possess a wide margin of safety when administered orally. The lack of mortality and the minimal clinical signs even at the maximum tolerated dose of 2000 mg/kg suggest that the compound has low acute systemic toxicity. The binding activity of the heterocyclic derivatives was initially evaluated using computational methods with the DPP-IV enzyme inhibitor. To validate these findings, the compounds were further tested for their animal activity on the HFD + low-dose induced diabetic rat model. Test compounds were studied at a dose of 45 mg/kg. Compared with the reference, alogliptin was used at a dose of 20 mg/kg. In the initial testing of antihyperglycemic activity, the heterocyclic derivatives were given orally. Blood glucose was recorded at 0–8 h at hourly intervals using a glucometer (BG-03) and compatible test strips. Blood samples were obtained from the retroorbital plexus. Percentage reductions in blood glucose from 0 to 8 h were calculated for the test compounds, all of which showed notable anti-diabetic activity, as presented in Table 6. The test compounds S1R7, S1R8, S1R2, S1R10, S2R7, S2R11, and S2R2 demonstrate more activity as compared to the reference alogliptin. The compounds S1R7 and S2R7 were investigated thoroughly, as they revealed the greatest percentage reduction in blood glucose levels, as shown in Figure 1.

Fasting blood glucose (FBG)

FBGL levels were recorded on days 7, 14, 21, and 28 during the 4-week study, as shown in Figure 2. A significant increase ($P < 0.01$) in FBGL was observed in rats subjected to the HFD combined with low-dose STZ, confirming the successful induction of diabetes when compared with the normal control group. Following treatment, the standard drug alogliptin produced a steady and marked reduction in FBGL across all time points. Similarly, rats treated with the test compounds S1R7 and S2R7 demonstrated a progressive and significant ($P < 0.01$) decline in FBG levels relative to the diabetic control group. By the end of the study, both test

Table 5: Toxicity assessment of the heterocyclic derivatives

Ligand	LD_{50} (mg/kg)	Hepatotoxicity	Carcinogenicity	Immunotoxicity	Mutagenicity	Cytotoxicity
S2R1	2301	-	-	-	-	-
S2R2	2506	-	-	-	-	-
S2R3	2304	-	-	-	-	-
S2R4	2543	-	-	-	-	-
S2R5	2487	-	-	-	-	-
S2R6	2694	-	-	-	-	-
S2R7	2562	-	-	-	-	-
S2R8	2681	-	-	-	-	-
S2R9	2498	-	-	-	-	-
S2R10	2653	-	-	-	-	-
S2R11	2574	-	-	-	-	-

Table 6: Percentage reduction in blood glucose levels for all test compounds

S. No.	Test compound	Percentage decrease in glucose levels	S. No.	Test compound	Percentage decrease in glucose levels
1	S1R1	56.2	13	S2R2	52.2
2	S1R2	82.7	14	S2R3	26.7
3	S1R3	55.6	15	S2R4	25
4	S1R4	60.2	16	S2R5	27.4
5	S1R5	55	17	S2R6	38.3
6	S1R6	54.1	18	S2R7	75.11
7	S1R7	88.2	19	S2R8	50.0
8	S1R8	85.1	20	S2R9	50
9	S1R9	29.8	21	S2R10	52.8
10	S1R10	75.6	22	S2R11	72.1
11	S1R11	38.8	23	Alogliptin	53.9
12	S2R1	58.2			

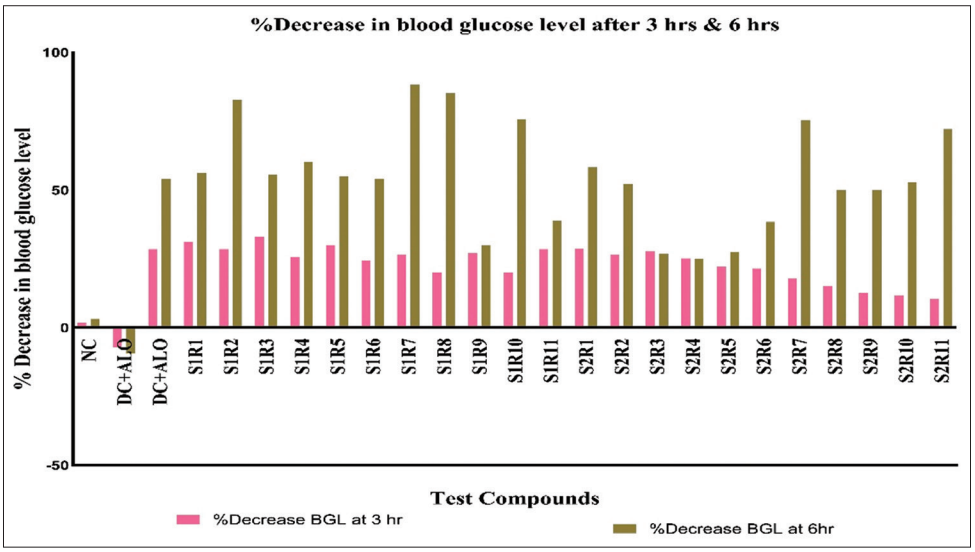

Figure 1: Blood glucose reduction (%) at 3 h and 6 h following treatment with S1R1–S2R11 and alogliptin in high-fat diet/streptozotocin diabetic rats

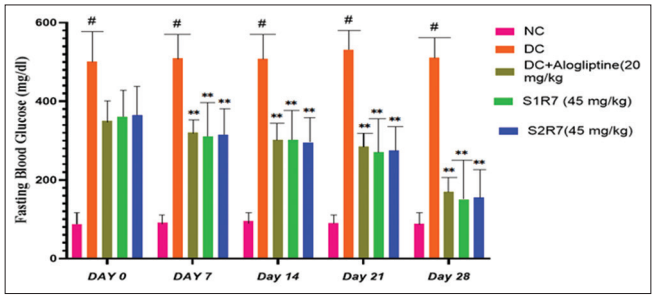

Figure 2: Fasting blood glucose level in high-fat diet/streptozotocin-induced diabetic rats following treatment with S1R7 and S2R7 (45 mg/kg) and the standard drug alogliptin (20 mg/kg)

compounds showed considerable antihyperglycemic activity, comparable to the standard treatment, indicating their potential effectiveness in controlling elevated blood glucose levels in diabetic rats.

OGTT

Figure 3 shows the effect of the test compounds S1R7 and S2R7 on blood sugar concentration during the OGTT in normal animals and HFD combined with low-dose STZ-induced diabetic animals. Baseline sugar levels were markedly higher in diabetic control rats relative to those of normal controls, confirming successful induction of hyperglycemia. After glucose administration, normal rats exhibited only a minor rise in blood glucose that gradually returned to baseline, whereas diabetic controls showed a pronounced and sustained peak from 15 to 120 min. Treatment with S1R7 and

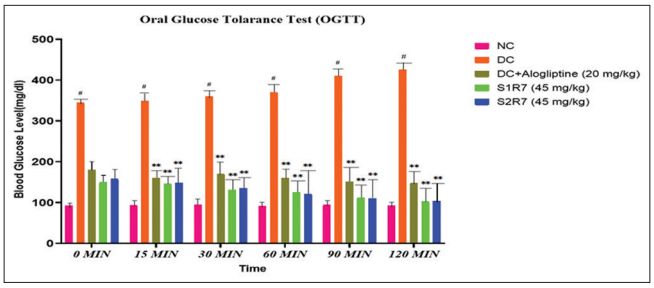

Figure 3: Oral glucose tolerance response in high-fat diet/streptozotocin-induced diabetic rats following treatment with S1R7 and S2R7 (45 mg/kg) and the standard drug alogliptin (20 mg/kg)

S2R7 resulted in an initial peak at 15 min, similar to diabetic controls, followed by a progressive decline in glucose levels, indicating improved glucose tolerance. By the end of the OGTT, the antihyperglycemic effect of S1R7 and S2R7 was against that of the reference drug alogliptin, highlighting their potential to reduce postprandial hyperglycemia effectively.

CONCLUSION

The combined computational and experimental findings strongly support the antidiabetic potential of the heterocyclic derivatives. Molecular docking studies revealed that several compounds, particularly S1R7, S1R8, S1R2, S1R10, S2R7, S2R11, and S2R2, exhibited strong binding affinity toward the DPP-IV enzyme, suggesting their potential to enhance incretin-mediated glucose regulation. These predictions were validated through *in vivo* studies. In the oral acute toxicity test, the selected derivatives were found to be safe at the tested doses, with no observable toxic effects. In the FBG evaluation, the active derivatives produced a significant and sustained reduction in blood sugar levels in HFD + low-dose STZ-induced diabetic rats. Similarly, in the OGTT, these compounds markedly improved glucose disposal, demonstrating better postprandial glucose control. Among all the derivatives, S1R7 and S2R7 consistently showed the highest antihyperglycemic activity, outperforming the standard drug alogliptin in lowering blood glucose and improving glucose tolerance. The improved pharmacodynamic response shows a strong correlation with the observed docking profiles. Overall, the study confirms that the integrated approach of molecular docking followed by *in vivo* validation is effective in identifying potent antidiabetic candidates. Compounds S1R7 and S2R7 emerge as the most promising leads for further development as DPP-IV inhibitors with superior antihyperglycemic efficacy.

ACKNOWLEDGMENTS

The authors would like to express their sincere gratitude to the Principal and Management of PES's Modern College of Pharmacy, Nigdi, Pune-44, for providing the necessary facilities and support to conduct this research work. The study was carried out without any external financial assistance from governmental, commercial, or non-profit funding agencies.

REFERENCES

1. Brito AK, Mendes AV, Timah Acha B, Santos Oliveira AS, Lopes Macedo J, Suzuki Cruzio A, *et al*. Experimental models of type 2 diabetes mellitus induced by combining hyperlipidemic diet (HFD) and streptozotocin administration in rats: An integrative review. Biomedicines 2025;13:1158.
2. Zhang M, Lv XY, Li J, Xu ZG, Chen L. The characterization of high-fat diet and multiple low-dose streptozotocin induced type 2 diabetes rat model. Exp Diabetes Res 2008;2008:704045.
3. Srinivasan K, Viswanad B, Asrat L, Kaul CL, Ramarao P. Combination of high-fat diet-fed and low-dose streptozotocin-treated rat: A model for type 2 diabetes and pharmacological screening. Pharmacol Res 2005;52:313-20.
4. Sugano M, Yamato H, Hayashi T, Ochiai H, Kakuchi J, Goto S, *et al*. High-fat diet in low-dose-streptozotocin-treated heminephrectomized rats induces all features of human type 2 diabetic nephropathy: A new rat model of diabetic nephropathy. Nutr Metab Cardiovasc Dis 2006;16:477-84.
5. Zardecki C, Dutta S, Goodsell DS, Voigt M, Burley SK. RCSB Protein Data Bank: A resource for chemical, biochemical, and structural explorations of large and small biomolecules. J Chem Educ 2016;93:569-75.
6. Naim MJ, Alam O, Alam MJ, Shaquiquzzaman M, Alam MM, Naidu VG. Synthesis, docking, *in vitro* and *in vivo* antidiabetic activity of pyrazole-based 2,4-thiazolidinedione derivatives as PPAR-γ modulators. Archiv Pharm (Weinheim) 2018;351:e1700223.
7. Sastry GM, Adzhigirey M, Day T, Annabhimoju R, Sherman W. Protein and ligand preparation: Parameters, protocols, and influence on virtual screening enrichments. J Comput Aided Mol Des 2013;27:221-34.
8. Sawant RL, Wadekar JB, Kharat SB, Makasare HS. Targeting PPAR-γ to design and synthesize antidiabetic thiazolidines. EXCLI J 2018;17:598-607.
9. Mohammad BD, Baig MS, Bhandari N, Siddiqui FA, Khan SL, Ahmad Z, *et al*. Heterocyclic compounds as dipeptidyl peptidase-IV inhibitors with special emphasis on oxadiazoles as potent anti-diabetic agents. Molecules 2022;27:6001.
10. Halgren TA, Murphy RB, Friesner RA, Beard HS, Frye LL, Pollard WT, *et al*. Glide: A new approach for rapid, accurate docking and scoring. 2. Enrichment factors in database screening. J Med Chem 2004;47:1750-9.
11. Almalki NA, Al-Abbasi FA, Moglad E, Afzal M, Al-Qahtani SD, Alzarea SI, *et al*. Protective activity of hirsutidin in high-fat intake and streptozotocin-induced

diabetic rats: *In silico* and *in vivo* study. Heliyon 2024;10:e38625.
12. Kar S, Leszczynski J. Open access *in silico* tools to predict the ADMET profiling of drug candidates. Expert Opin Drug Discov 2020;15:1473-87.
13. Egan WJ, Merz KM Jr., Baldwin JJ. Prediction of drug absorption using multivariate statistics. J Med Chem 2000;43:3867-77.
14. Lipinski CA, Lombardo F, Dominy BW, Feeney PJ. Experimental and computational approaches to estimate solubility and permeability in drug discovery and development settings. Adv Drug Deliv Rev 2012;64:4-17.
15. Banerjee P, Kemmler E, Dunkel M, Preissner R. ProTox 3.0: A webserver for the prediction of toxicity of chemicals. Nucleic Acids Res 2024;52:W513-20.
16. Sharma A, Narang A, Kumar N, Rana R, Megha, Pooja, *et al*. CADD based designing and biological evaluation of novel triazole based thiazolidinedione coumarin hybrids as antidiabetic agent. Sci Rep 2025;15:4302.
17. Konsue A, Picheansoonthon C, Talubmook C. Fasting blood glucose levels and hematological values in normal and streptozotocin-induced diabetic rats of Mimosa pudica L. Extracts. Pharmacogn J 2017;9:315-22.
18. World Health Organization. Definition and Diagnosis of Diabetes Mellitus and Intermediate Hyperglycaemia. Geneva, Switzerland: World Health Organization; 2006. p. 17-20.

Source of Support: Nil. **Conflicts of Interest:** None declared.